# Preparation and Characterisation of Some Dimeric η²-Diyne Complexes of Cobalt

Catherine E. Housecroft,[a] Brian F. G. Johnson,[*,b] Muhammad S. Khan,[a] Jack Lewis,[a] Paul R. Raithby,[a] Michael E. Robson[a] and Della A. Wilkinson[a]

[a] University Chemical Laboratory, Lensfield Road, Cambridge CB2 1EW, UK

[b] Department of Chemistry, University of Edinburgh, West Mains Road, Edinburgh EH9 3JJ, UK

The organometallic dimers [{$Co_2(CO)_6$}$_2$(diyne)] (diyne = $HC_2C_6H_4C_2H$ **1**, $HC_2C_6H_4C_6H_4C_2H$ **2**, $HC_2C_6H_4CH_2C_6H_4C_2H$ **3**, $Me_3SiC_2C_6H_4C_6H_4C_2SiMe_3$ **4**, $Me_3SiC_2C_6H_4CH_2C_6H_4C_2SiMe_3$ **5** or $Me_3SnC_2C_6H_4C_6H_4C_2SnMe_3$ **6**) have been synthesised from the reaction of octacarbonyldicobalt(0), [$Co_2(CO)_8$], with the appropriate diyne. The products have been characterised by infrared spectroscopy, electron impact (EI) mass spectrometry, microanalysis and $^1H$ NMR spectroscopy. The complexes **1**, **3** and **4** have been characterised by single-crystal X-ray crystallography. In all cases both 'yne' fragments of the diyne bond to a $Co_2(CO)_6$ fragment with the C≡C vector essentially perpendicular to the Co–Co vector. A bonding analysis by a Fenske–Hall calculation using the crystallographically determined co-ordinates for dimer **1** is consistent with the observed distortion of the $Co_2C_2$ bonding pattern away from quasi-tetrahedral geometry.

We are currently interested in the chemistry of polymeric materials which contain clusters supported on a carbon backbone. We have previously reported[1] the synthesis and full characterisation of the dimer [{$Co_2(CO)_6(PhC_2)$}$_2$]. In this paper we report more extensive studies into a series of related dimers, of general formula [$Co(CO)_6$(diyne)] (diyne = $HC_2C_6H_4C_2H$ **1**, $HC_2C_6H_4C_6H_4C_2H$ **2**, $HC_2C_6H_4CH_2C_6$-$H_4C_2H$ **3**, $Me_3SiC_2C_6H_4C_6H_4C_2SiMe_3$ **4**, $Me_3SiC_2C_6H_4$-$CH_2C_6H_4C_2SiMe_3$ **5** or $Me_3SnC_2C_6H_4C_6H_4C_2SnMe_3$ **6**. Similar polymers containing the [$Co_2(CO)_6C_2$] unit have been reported previously.[2,3] Thus, Magnus and Becker[3] synthesised the dimers [{$Co_2(CO)_6(Me_3SiC_2)$}$_2$] and [{$Co_2(CO)_6$}$_2$($Me_3$-$SiC_2C_2H$)] which contain two linked [$Co_2(CO)_6C_2$] units and are clearly relevant to the work discussed here. More recently, the compound [$Co_2(CO)_6(Me_3SiC_2H)$] has been reported[4] to undergo oxidative coupling to generate a hexacobalt complex of cyclo[18]carbon.

## Results and Discussion

The organometallic dimers [{$Co_2(CO)_6$}$_2$(diyne)] (diyne = $HC_2C_6H_4C_2H$ **1**, $HC_2C_6H_4C_6H_4C_2H$ **2**, $HC_2C_6H_4CH_2$-$C_6H_4C_2H$ **3**, $Me_3SiC_2C_6H_4C_6H_4C_2SiMe_3$ **4**, $Me_3SiC_2C_6H_4$-$CH_2C_6H_4C_2SiMe_3$ **5** or $Me_3SnC_2C_6H_4C_6H_4C_2SnMe_3$ **6**) have been synthesised from the reaction of two molar equivalents of octacarbonyldicobalt(0), [$Co_2(CO)_8$], with the appropriate diyne in hexane at room temperature. In the case of the diynes $HC_2C_6H_4C_6H_4C_2H$, $HC_2C_6H_4CH_2C_6H_4C_2H$ and $Me_3SiC_2C_6H_4C_6H_4C_2SiMe_3$ higher yields of the products were obtained when the reaction was carried out at 40 °C. In all cases the reactions were monitored by following the disappearance of the signals due to the bridging carbonyls of [$Co_2(CO)_8$], in the IR spectra. The only other product of the reaction appeared to be carbon monoxide. The products were purified by filtration through a column of Celite, followed by crystallisation from the filtrate at 0 °C to give dark red microcrystalline solids. The products are not air-sensitive as solids but slowly decompose to uncharacterised materials in hexane solution.

The products were characterised by IR spectroscopy, electron impact (EI) mass spectrometry, microanalysis and $^1H$ NMR spectroscopy. In the case of the complexes **1**, **3** and **4** the characterisations have been confirmed and the molecular geometries established by single-crystal X-ray crystallography.

The IR spectra of the complexes **1–6** all show the characteristic carbonyl pattern observed for previously reported cobalt–alkyne compounds[5] with six bands in the terminal carbonyl stretching region. Since these spectra and those of known cobalt–alkyne derivatives are very similar it is reasonable to conclude that a similar co-ordination mode for the alkyne is adopted but in this case that both alkyne linkages are co-ordinated to cobalt atoms. The molecule should therefore have overall $C_2$ symmetry. On this basis, twelve $\nu_{CO}$ bands are expected in contrast to the six observed. It would appear, therefore, that there is little or no vibrational coupling between the two independent {$Co_2(CO)_6C_2$} units, and consequently, a $C_{2v}$ symmetry for the local environment in each of the {$Co_2(CO)_6C_2$} moieties may be invoked to explain the observed IR pattern. No $\nu_{C≡C}$ stretches were observed in the region of 2100 cm$^{-1}$, and more importantly, no C–H stretch (expected at 3290 cm$^{-1}$) was present. This we take to indicate the absence of a C≡C triple bond consistent with the view that both alkyne linkages are co-ordinated to $Co_2$ units.

For the complexes **1**, **3** and **5** the EI mass spectra showed the respective molecular ions, as well as peaks corresponding to the consecutive loss of the twelve carbonyl ligands. The observed isotopic distributions are fully consistent with those simulated for the appropriate stoichiometry [{$Co_2(CO)_6$}$_2$(diyne)], although the peak representing the diyne fragment could not be distinguished in the low molecular weight region. Microanalytical data were also consistent with the empirical formulae $C_{11}H_3Co_2O_6$, $C_{29}H_{12}Co_4O_{12}$ and $C_{35}H_{28}Co_4O_{12}Si_2$, respectively.

The EI mass spectra for the remaining complexes **2**, **4** and **6** were less conclusive. For the proposed complex **2** the only fragment identified was at m/z 202, which corresponds to the diyne ligand. However, microanalytical data support the suggested empirical formulae, $C_{14}H_5Co_2O_6$. For complex **4** the EI mass spectrum did not show the parent ion, however, peaks were observed at m/z 844 and 771 which correspond to the molecular fragments [{$Co_2(CO)_6$}$_2$($Me_3SiC_2C_6H_4C_6H_4C_2$)]$^+$ and
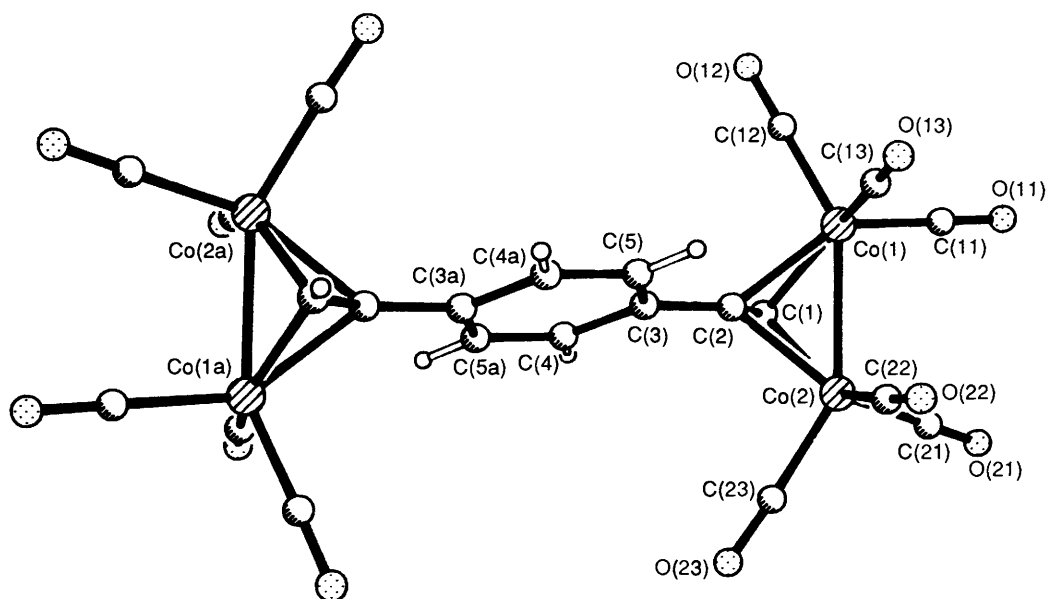
**Fig. 1** The molecular structure of [{Co₂(CO)₆}₂(HC₂C₆H₄C₂H)] **1** showing the atom numbering scheme

**Table 1** Selected bond lengths (Å) and angles (°) for [{Co₂(CO)₆}₂-(HC₂C₆H₄C₂H)] **1**

| Co(1)–Co(2) | 2.468(1) | Co(1)–C(1) | 1.944(7) |
|---|---|---|---|
| Co(1)–C(2) | 1.975(6) | Co(2)–C(1) | 1.946(9) |
| Co(2)–C(2) | 1.966(6) | C(1)–C(2) | 1.334(9) |
| C(2)–C(3) | 1.436(8) | | |
| | | | |
| Co(2)–Co(1)–C(1) | 50.6(3) | Co(2)–Co(1)–C(2) | 51.0(2) |
| C(1)–Co(1)–C(2) | 39.8(3) | Co(2)–Co(1)–C(1) | 50.6(2) |
| Co(1)–Co(2)–C(2) | 51.4(2) | C(1)–Co(2)–C(2) | 39.9(3) |
| Co(1)–C(1)–Co(2) | 78.8(3) | Co(1)–C(1)–C(2) | 71.4(4) |
| Co(2)–C(1)–C(2) | 70.9(5) | Co(1)–C(2)–Co(2) | 77.6(3) |
| Co(1)–C(2)–C(1) | 68.9(4) | Co(2)–C(2)–C(1) | 69.3(4) |
| Co(1)–C(2)–C(3) | 136.9(4) | Co(2)–C(2)–C(3) | 133.4(5) |
| C(1)–C(2)–C(3) | 141.9(7) | | |

[{Co₂(CO)₆}₂(C₂C₆H₄C₆H₄C₂)]⁺ respectively. Peaks corresponding to the loss of twelve carbonyl ligands were also observed indicating that two {Co₂(CO)₆} moieties have co-ordinated to the diyne. However, microanalytical data were again consistent with the proposed molecular formula [{Co₂(CO)₆}₂(Me₃SiC₂C₆H₄C₆H₄C₂SiMe₃)]. The EI mass spectrum of **6** was also inconclusive and the microanalytical data showed poor agreement with calculated values for the proposed stoichiometry, C₃₀H₂₆Co₄O₁₂Sn₂. This we believe is due to small amounts of complex **2** which could not be successfully removed.

*Crystal and Molecular Structure of* [{Co₂(CO)₆}₂(HC₂C₆-H₄C₂H)] **1**.—The crystal structure of **1** consists of discrete molecules of [{Co₂(CO)₆}₂(HC₂C₆H₄C₂H)] in which the two Co₂(CO)₆(alkyne) fragments are linked by the aryl group. The molecules are separated by normal van der Waals distances.

The molecular structure of **1** is shown in Fig. 1, while selected bond parameters are listed in Table 1. The molecule sits on a crystallographic centre of symmetry which lies at the centre of the aryl ring. The 'Co₂C₂' core adopts a pseudo-tetrahedral geometry with the C(1)–C(2) alkyne bond lying essentially perpendicular to the Co(1)–Co(2) vector. Each of the cobalt atoms is also co-ordinated to three terminal carbonyl ligands which display linear geometries. The linking aryl group is bonded to one of the alkylenic carbon atoms, C(2), and exhibits a twist with respect to the C(1)–C(2) vector [C(1)–C(2)–C(3)–C(4) 16.1, C(1)–C(2)–C(3)–C(5) −165.8°].

The Co(1)–Co(2) bond length found in **1** lies within the range 2.460–2.477 Å observed for other dicobalt systems that are bridged by perpendicular alkyne ligands,[1,6–8] but is shorter than the value of 2.52 Å found for the Co–Co distance in the parent carbonyl, [Co₂(CO)₈].[9] The C(1)–C(2) length is also within the range 1.33–1.36 Å of values for the alkylenic C–C bond in the same set of related dicobalt complexes.[1,6–8] This C–C distance shows a lengthening of ca. 0.15 Å from the value of 1.18 Å found in the free alkyne, an observation that is consistent with the delocalisation of electron density into the Co₂ unit.

The most interesting feature of the structure of **1** is the asymmetry of the Co–C distances in the 'Co₂C₂' core. These four distances may be divided into two sets which are inequivalent to within experimental error (at the 2.5σ level). The two Co–C(1) distances average ca. 1.94 Å, while the Co–C(2) are longer, with an average distance of 1.97 Å. Thus, the 'Co₂C₂ pseudo-tetrahedron' is distorted with the longer Co–C(alkyne) interactions being associated with the alkylenic carbon co-ordinated to the central phenylene group. This structural feature is in contrast with the data for [Co₂(CO)₆(alkyne)] complexes where the alkyne is symmetrically substituted, and the four Co–C distances are equal to within experimental error.[7]

*Crystal and Molecular Structure of* [{Co₂(CO)₆}₂(Me₃Si-C₂C₆H₄C₆H₄C₂SiMe₃)] **4**.—The crystal structure of **4** consists of discrete molecules of [{Co₂(CO)₆}₂(Me₃SiC₂C₆H₄C₆H₄C₂-SiMe₃)] separated by normal van der Waals distances.

The molecular structure of **4** is shown in Fig. 2 and selected bond lengths and angles are listed in Table 2. The dimeric molecule lies on a crystallographic two-fold symmetry axis located at the midpoint of the C(9)–C(9a) bond, and the overall molecular geometry is similar to that observed for **1**. The dihedral angle between the two symmetry related aryl groups is 20.0°; this small twist reduces the steric interaction between the hydrogen atoms on the two rings. The aryl group, which is co-ordinated to one of the alkylenic carbon atoms, C(2), also shows a small twist with respect to the alkylenic C(1)–C(2) vector [C(1)–C(2)–C(6)–C(7) −16.1, C(1)–C(2)–C(6)–C(11) 167.4°] similar to that found in **1**. As expected the C(1)–C(2)–C(3) bond angle, 142.9(8)°, and the C(2)–C(1)–Si(1) bond angle, 147.6(8)°, are greatly reduced from the 180° observed for linear alkynes. The length of the C(9)–C(9a) bond [1.50(2) Å], linking the two aryl groups, provides little evidence of delocalisation of electron density between the aromatic rings.

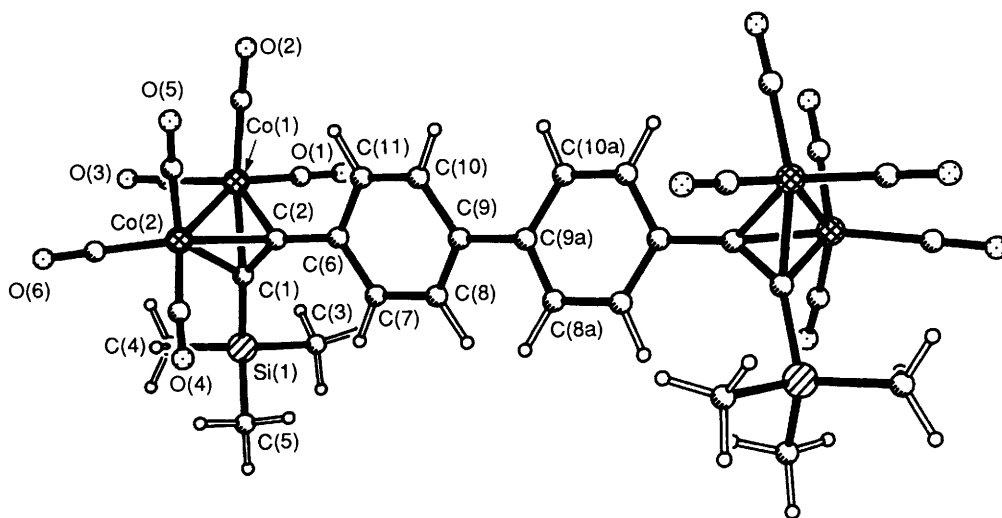The Co–Co distance of 2.477(2) Å found in **4** is slightly longer

**Fig. 2** The molecular structure of [{Co₂(CO)₆}₂(Me₃SiC₂C₆H₄C₆H₄C₂SiMe₃)] **4** showing the atom numbering scheme

**Table 2** Selected bond lengths (Å) and angles (°) for [{Co₂(CO)₆}₂-(Me₃SiC₂C₆H₄C₆H₄C₂SiMe₃)] **4**

| | | | |
|---|---|---|---|
| Co(1)–Co(2) | 2.477(2) | Co(1)–C(1) | 1.994(8) |
| Co(1)–C(2) | 1.982(8) | Co(2)–C(1) | 2.003(9) |
| Co(2)–C(2) | 1.964(9) | C(1)–C(2) | 1.335(12) |
| C(1)–Si(1) | 1.850(8) | C(2)–C(6) | 1.456(13) |
| C(9)–C(9a) | 1.504(18) | | |
| | | | |
| C(1)–Co(1)–Co(2) | 51.9(3) | C(2)–Co(1)–Co(2) | 50.8(3) |
| C(2)–Co(1)–C(1) | 39.2(3) | C(1)–Co(2)–Co(1) | 51.5(2) |
| C(2)–Co(2)–Co(1) | 51.4(2) | C(2)–Co(2)–C(1) | 39.3(4) |
| Co(2)–C(1)–Co(1) | 76.6(3) | C(2)–C(1)–Co(1) | 69.9(5) |
| C(2)–C(1)–Co(2) | 68.8(5) | Si(1)–C(1)–Co(1) | 131.6(4) |
| Si(1)–C(1)–Co(2) | 133.1(5) | Si(1)–C(1)–C(2) | 147.6(8) |
| Co(2)–C(2)–Co(1) | 77.8(3) | C(1)–C(2)–Co(1) | 70.9(5) |
| C(1)–C(2)–Co(2) | 71.9(6) | C(6)–C(2)–Co(1) | 134.9(6) |
| C(6)–C(2)–C(2) | 131.1(6) | C(6)–C(2)–C(1) | 142.9(8) |

than the value found in **1** but still lies within the expected range for this class of complex. The C≡C bond length, 1.34(1) Å, is again consistent with the lengthening of the bond due to loss of triple-bond character and is similar to the value observed in [{Co₂(CO)₆}₂(HC₂C₆H₄C₂H)] **1**.

An analysis of the four Co–C(alkyne) distances in **4** shows that they are not significantly different at the 2.5σ level. However, these distances may be divided into two groups, with the average Co–C(1) distance (2.00 Å) being *ca.* 0.03 Å longer than the average Co–C(2) distance (1.97 Å). If this trend is real, the longer Co–C(alkyne) distances are associated with the carbon co-ordinated to the SiMe₃ group, in contrast to the structure of **1**, when the longer distances were associated to the phenylene co-ordinated alkylenic carbon atom. This feature may be related to the relative steric requirements of the SiMe₃ group in **4**, compared to that of an H atom in **1**.

*Crystal and Molecular Structure of* [{Co₂(CO)₆}₂(HC₂-C₆H₄CH₂C₆H₄C₂H)] **3**.—The crystal structure of **3** consists of discrete molecules of [{Co₂(CO)₆}₂(HC₂C₆H₄CH₂C₆H₄C₂H)] separated by normal van der Waals distances. However, the asymmetric unit within the cell contains two independent but structurally similar molecules.

The structure of one of the independent molecules of **3** is shown in Fig. 3 while selected bond parameters for both molecules are listed in Table 3. The overall molecular geometry resembles that found in complexes **1** and **4**, except that the introduction of the methylene group between the two aryl

groups results in a greater twist in the carbon backbone and eliminates the possibility of any long-range delocalisation between the aryl rings; the two aryl ring planes make an angle of 84.1°. The bond angle C(2)–C(1)–C(10), at 115.8(6)° [114.6(7)° in molecule 2], is significantly larger than the idealised angle of 109.5° for sp³ hybridised carbon, but it is the steric requirements of the bulky substituent groups that cause this increase in angle to reduce the strain. The relative orientation of the two halves of the molecule is illustrated by the space-filling diagram shown in Fig. 4.

The four unique Co–Co distances for the two independent molecules for **3** lie in the range 2.461(2)–2.470(2) Å, which is close to the values found in **1** and **4**, and to metal–metal distances in other related systems.[1,6–8] The four unique alkylenic C–C bonds [average length 1.34(2) Å] also lie in the expected range for alkyne groups co-ordinated to 'Co₂(CO)₆' units. The spread of Co–C(alkyne) distances [range 1.93(1)–1.99(1) Å], together with the relatively high estimated standard deviations associated with them, makes an analysis of the bonding within the Co₂(CO)₆ cores impossible; there are no clear cut sets of distances that can be associated with either the alkylenic carbon bonded to the hydrogen or the carbon bonded to the aryl ring as was found in complexes **1** and **4**. However, if the eight unique Co–C(alkyne-H) distances are averaged the value obtained (1.95 Å) is *ca.* 0.02 Å shorter than the value for the average of the eight unique Co–C(alkyne-aryl) distances (1.97 Å). This trend is the same as found in **1**, and so the bonding in **3** may be rationalised in the same manner.

*Proton NMR Spectroscopy.*—The ¹H NMR spectroscopic data for the complexes **1**–**6** (Table 4) are consistent with the overall geometry established in the solid state for complexes **1**, **3** and **4**, and with the IR spectroscopy studies.

For complexes **1**–**3**, which contain a terminal 'alkyne' hydrogen, a single resonance is observed in the region δ 6.20–6.28. As expected,[10,11] because of the reduction in the C≡C triple-bond character, there is a downfield shift in the position of these terminal protons with respect to the free ligand (δ 3.16).

All complexes have aromatic rings and consequently their ¹H NMR spectra contain peaks in the aromatic region (δ 7–8). For the complexes **1** and **4** the ¹H NMR spectra each contains a singlet in this region. For **1** the appearance of a singlet at δ 7.45 (integral 4 H) indicates that the four aromatic protons are equivalent and that the aromatic ring must be rotating about the C(2)–C(3) bond (Fig. 1). The resonance observed at δ 7.58 in the ¹H NMR spectrum of **4** also appears as a singlet. The ¹H NMR spectra for the remaining complexes reveal non-
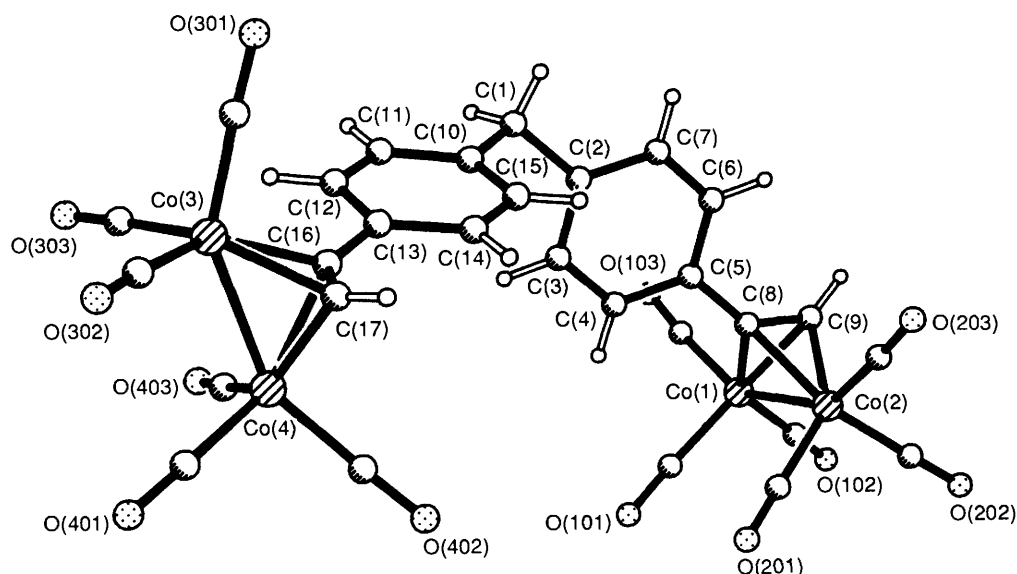
**Fig. 3** The molecular structure of [{Co₂(CO)₆}₂(HC₂C₆H₄CH₂C₆H₄C₂H)] 3 showing the atom numbering scheme

**Table 3** Selected bond lengths (Å) and angles (°) for [{Co₂(CO)₆}₂(HC₂C₆H₄CH₂C₆H₄C₂H)] 3

| Molecule 1 | | | | Molecule 2 | | | |
|---|---|---|---|---|---|---|---|
| Co(1)–Co(2) | 2.470(2) | Co(3)–Co(4) | 2.462(2) | Co(5)–Co(6) | 2.461(2) | Co(7)–Co(8) | 2.461(2) |
| Co(1)–C(8) | 1.954(10) | Co(3)–C(16) | 1.954(9) | Co(5)–C(25) | 1.981(8) | Co(7)–C(33) | 1.977(9) |
| Co(1)–C(9) | 1.951(11) | Co(3)–C(17) | 1.932(8) | Co(5)–C(26) | 1.957(8) | Co(7)–C(34) | 1.944(10) |
| Co(2)–C(8) | 1.985(7) | Co(4)–C(16) | 1.983(10) | Co(6)–C(25) | 1.982(10) | Co(8)–C(33) | 1.959(9) |
| Co(2)–C(9) | 1.944(8) | Co(4)–C(17) | 1.977(11) | Co(6)–C(26) | 1.954(10) | Co(8)–C(34) | 1.930(10) |
| C(8)–C(9) | 1.329(13) | C(16)–C(17) | 1.349(11) | C(25)–C(26) | 1.351(14) | C(33)–C(34) | 1.319(9) |
| C(5)–C(8) | 1.461(12) | C(13)–C(16) | 1.462(12) | C(22)–C(25) | 1.449(14) | C(30)–C(33) | 1.454(10) |
| | | | | | | | |
| Co(2)–Co(1)–C(8) | 51.7(2) | Co(4)–Co(3)–C(16) | 51.8(3) | Co(6)–Co(5)–C(25) | 51.6(3) | Co(8)–Co(7)–C(33) | 51.0(2) |
| Co(2)–Co(1)–C(9) | 50.2(2) | Co(4)–Co(3)–C(17) | 51.8(3) | Co(6)–Co(5)–C(26) | 103.3(6) | Co(8)–Co(7)–C(34) | 50.3(3) |
| C(8)–Co(1)–C(9) | 39.8(4) | C(16)–Co(3)–C(17) | 40.6(3) | C(25)–Co(5)–C(26) | 40.1(4) | C(33)–Co(7)–C(34) | 39.3(3) |
| Co(1)–Co(2)–C(8) | 50.6(3) | Co(3)–Co(4)–C(16) | 50.8(3) | Co(5)–Co(6)–C(25) | 51.6(2) | Co(7)–Co(8)–C(33) | 51.6(3) |
| Co(1)–Co(2)–C(9) | 50.8(3) | Co(3)–Co(4)–C(17) | 50.2(3) | Co(5)–Co(6)–C(26) | 51.1(2) | Co(7)–Co(8)–C(34) | 50.8(3) |
| C(8)–Co(2)–C(9) | 39.5(4) | C(16)–Co(4)–C(17) | 39.8(3) | C(25)–Co(6)–C(26) | 40.2(4) | C(33)–Co(8)–C(34) | 39.6(3) |
| Co(1)–C(8)–Co(2) | 77.7(3) | Co(3)–C(16)–C(17) | 68.8(5) | Co(5)–C(25)–Co(6) | 76.8(4) | Co(7)–C(33)–C(34) | 69.0(6) |
| Co(1)–C(8)–C(9) | 70.0(6) | Co(4)–C(16)–C(17) | 69.8(6) | Co(5)–C(25)–C(26) | 69.0(5) | Co(8)–C(33)–C(34) | 69.0(5) |
| Co(2)–C(8)–C(9) | 71.9(5) | Co(3)–C(16)–Co(4) | 77.4(3) | Co(6)–C(25)–C(26) | 68.8(6) | Co(7)–C(33)–Co(8) | 77.4(3) |
| Co(1)–C(9)–Co(2) | 78.7(4) | Co(3)–C(17)–C(16) | 70.6(5) | Co(5)–C(26)–Co(6) | 78.0(4) | Co(7)–C(34)–C(33) | 71.7(6) |
| Co(1)–C(9)–C(8) | 70.2(6) | Co(4)–C(17)–C(16) | 70.3(6) | Co(5)–C(26)–C(25) | 70.9(5) | Co(8)–C(34)–C(33) | 71.4(6) |
| Co(2)–C(9)–C(8) | 71.9(5) | Co(3)–C(17)–Co(4) | 78.1(3) | Co(6)–C(26)–C(25) | 71.1(6) | Co(7)–C(34)–Co(4) | 78.9(4) |
| C(5)–C(8)–C(9) | 140.9(9) | | | C(22)–C(25)–C(26) | 142.5(9) | | |
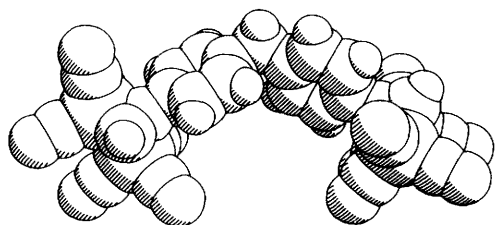


**Fig. 4** A space filling diagram for [{Co₂(CO)₆}₂(HC₂C₆H₄CH₂-C₆H₄C₂H)] 3 showing the orientation of the two Co₂(CO)₆ fragments

equivalent aromatic protons, and show simple splitting patterns characteristic of AB systems.

In the ¹H NMR spectrum of 2 there are four peaks in the aromatic region. This is because the resonances of the two types of aromatic protons are split due to mutual coupling. Since $\delta_A - \delta_B$ (17.3 Hz) is of comparable magnitude to the coupling constant, $J_{AB}$ (7.5 Hz), the first-order approximation usually employed for assigning spin–spin coupling patterns no longer holds. Line perturbations arising from this effect result in four

signals which are not of equal intensity. Instead, the four signals appear as doublets where one resonance from each has been enhanced at the expense of the other band. For the doublet arising from proton 3 the lower field resonance is enhanced, whereas for proton 2 the higher field resonance is bigger. The splitting pattern is quite extreme as the lines are very perturbed. The splitting $J_{AB}$ is 7.5 Hz; this is typical for adjacent protons on an aromatic ring.[12] It is possible to assign the downfield doublet to the proton closest to the {Co₂(CO)₆C₂} moiety by comparison with the spectrum of [Co₂(CO)₆(PhC₂Ph)].

In contrast, the aromatic region in the ¹H NMR spectrum of 3 contains signals easily assigned to an AB system. The non-equivalent aromatic protons give rise to two doublets where $\delta_A$ is at 7.36 for H² and $\delta_B$ is at 6.82 for H³. Convincing evidence for the formation of complex 6 comes from its ¹H NMR spectrum which exhibits a simple AB splitting pattern in the aromatic region and a singlet at δ 0.49. The aromatic signals did, however, prove difficult to distinguish because of line perturbations arising from second order effects.

Two of the complexes, 3 and 5, which possess methylene protons exhibit a singlet at δ 3.91 in their ¹H NMR spectra,

**Table 4** Proton NMR[a] chemical shifts for [{Co$_2$(CO)$_6$}$_2$(diyne)] 1–6

| Complex | Diyne | Terminal atom/group | | Aromatic protons | –CH$_2$– |
| | | H | EMe$_3$ | | |
|---|---|---|---|---|---|
| 1 | HC$_2$C$_6$H$_4$C$_2$H[b] | 6.25 (s, 2 H) | | 7.45 (s) | |
| 2 | HC$_2$C$_6$H$_4$C$_6$H$_4$C$_2$H[b] | 6.28 (s, 2 H) | | 7.59 (AB, $J_{AB}$ = 10 Hz, 8 H), 7.52 | |
| 3 | HC$_2$C$_6$H$_4$CH$_2$C$_6$H$_4$C$_2$H[c] | 6.20 (s, 2 H) | | 7.45 (AB, $J_{AB}$ = 7.5 Hz, 8 H), 7.09 | 3.91 (s, 2 H) |
| | | 5.78 (s, 2 H) | | 7.36 (AB, $J_{AB}$ = 7.5 Hz, 8 H), 6.82 | 3.53 (s, 2 H) |
| 4 | Me$_3$SiC$_2$C$_6$H$_4$C$_6$H$_4$C$_2$SiMe$_3$ | | 0.43 (s, 18 H) | 7.58 (s, 8 H) | |
| 5 | Me$_3$SiC$_2$C$_6$H$_4$CH$_2$C$_6$H$_4$C$_2$SiMe$_3$ | | 0.42 (s, 18 H) | 7.50 (AB, $J_{AB}$ = 7.5 Hz, 8 H), 7.12 | 3.91 (s, 2 H) |
| 6 | Me$_3$SnC$_2$C$_6$H$_4$C$_6$H$_4$C$_2$SnMe$_3$ | | 0.49 (s, 18 H, $J_{SnH}$ = 25 Hz) | 7.57 (AB, $J_{AB}$ = 5 Hz, 8 H), 7.52 | |

[a] In CDCl$_3$, 250 MHz at 20 °C unless otherwise stated. [b] In C$_6$D$_{12}$. [c] In C$_6$D$_6$.

**Table 5** Mulliken overlap populations (% values in parentheses) for orbital interactions between the fragments Co$_2$(CO)$_6$ and PhCCH in the model compound [Co$_2$(CO)$_6$(PhCCH)], total Mullikan overlap population = 0.664

| MO of the Co$_2$(CO)$_6$ fragment | MO of the PhCCH fragment | | | | | | |
| | 16 | 18 | 19(HOMO) | 20(LUMO) | 21 | 22 | 23 |
|---|---|---|---|---|---|---|---|
| 38 | | | | 0.145 (22) | 0.013 (2) | 0.036 (5) | |
| 39(HOMO) | | | | 0.026 (4) | 0.013 (2) | 0.068 (10) | 0.045 (7) |
| 40(LUMO) | 0.024 (4) | 0.129 (19) | 0.012 (2) | | | | |
| 41 | 0.018 (3) | 0.024 (4) | 0.083 (12) | | | | |
| 42 | | 0.028 (4) | | | | | |



MO's (40-18)    MO's (38-20)
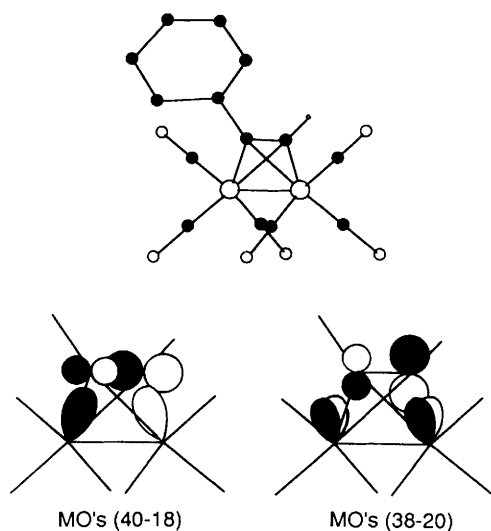
**Fig. 5** The two major interactions of the Co$_2$(CO)$_6$ fragment with the asymmetrical alkyne PhCCH

unchanged from the observed signal for the free ligand. The $^1$H NMR spectrum of **5** is almost identical to that observed for the complex **4**, the only difference arising from the central CH$_2$ group which results in an additional peak in the proton NMR at δ 3.91.

The $^1$H NMR spectrum of complex **4** is simple. A singlet due to the aromatic protons is observed at δ 7.58 (integral 8 H) together with a high-field singlet at δ 0.43 (integral 18 H) for the protons of the trimethylsilyl group. The methyl protons are equivalent and significantly shielded by the adjacent silicon atom. They appear slightly downfield from methyl protons of a *tert*-butyl group joined to a carbon atom (δ 0.9)[12] but from a comparison with the chemical shifts for the methyl protons in the compounds [{Co$_2$(CO)$_6$(C$_2$SiMe$_3$)}$_2$] (δ 0.35)[13] and [Me$_2$Si{Co$_2$(CO)$_6$C$_2$Ph}$_2$] (δ 0.90)[14] it is clear that they are in the typical region for protons in this type of environment.

The $^1$H NMR spectrum of complex **6** contains the expected aromatic singlet at δ 7.57 and a singlet corresponding to the SnMe$_3$ at high field. It is possible to calculate the extent of contamination by complex **2** from a comparison of the integrals

arising from the SnMe$_3$ group with that of the terminal hydride signal in **2**. The ratio of these two peaks is *ca.* 1 : 100. One other feature of this spectrum is the presence of satellites where due to $^{119}$Sn-$^1$H spin-spin coupling, $J_{Sn-H}$ = 25 Hz. The resonances show little change from those seen in the free ligand.

*Fenske-Hall Calculations.*—The bonding within the cluster [Co$_2$(CO)$_6$(HCCH)] has previously been analysed by one of us[15] and indeed the frontier orbitals of the Co$_2$(CO)$_6$ fragment are well documented.[16] For these reasons, the discussion below centres only on the features of the bonding in the model compound [Co$_2$(CO)$_6$(HCCPh)] which are responsible for the distortion of the Co$_2$C$_2$ core observed experimentally in [{Co$_2$(CO)$_6$}$_2${HCCC$_6$H$_4$CCH}] [Co–C 1.975(6), 1.966(6) Å compared with 1.947(9) and 1.946(9) Å]. The bonding is described in terms of the interaction of the Co$_2$(CO)$_6$ fragment with phenylacetylene. Prior to co-ordination to the dimetal centre, the substituents of the alkyne bend back. As expected, the nature of some of the frontier MOs reflects the asymmetric nature of the alkyne. The lowest unoccupied molecular orbital (LUMO) has C–C π* character (35% for C$_H$ and 24% for C$_{Ph}$) and is significantly stabilised from its position as the third lowest lying unoccupied MO in linear PhC≡CH. Table 5 lists Mulliken overlap populations for the interfragment interactions and indicates the importance of each interaction in terms of its percentage of the total Mullikan overlap population. The major orbital interactions between {Co$_2$(CO)$_6$} and {PhCCH} are: (38–20), (39–22), (40–18) and (41–19). Of the alkyne MOs involved 18–21, MOs 18, 19 and 20 exhibit a significantly greater C$_H$ than C$_{Ph}$ character. The frontier orbitals of the Co$_2$(CO)$_6$ fragment are symmetrical with respect to a plane bisecting the Co–Co vector but any asymmetry in the MOs of the alkyne will cause distortion in the resultant MOs of [Co$_2$(CO)$_6$(PhCCH)]. Two of the major interactions are drawn schematically in Fig. 5 and each leads to a greater Co–C$_H$ overlap than Co–C$_{Ph}$. Of the total cluster bonding, 67% of it involves MOs in which the Co–C$_H$ interactions are dominant over Co–C$_{Ph}$ interactions. Hence, the bonding analysis is consistent with the experimental observation that the Co–C$_H$ bonds are shorter than the Co–C$_{aryl}$ bonds in [{Co$_2$(CO)$_6$}$_2${HCCC$_6$H$_4$CCH}].

In conclusion, it is worthy of note that the preparation of **6** is in contrast to the report[17] that the diyne Me$_3$(SnC$_2$Ph)$_2$

**Table 6** Crystal data, data collection, and processing parameters for complexes **1**, **3** and **4**

| Complex | 1 | 3 | 4 |
|---|---|---|---|
| Formula | $C_{22}H_6Co_4O_{12}$ | $C_{29}H_{12}Co_4O_{12}$ | $C_{34}H_{26}Co_4O_{12}Si_2$ |
| $M$ | 698.02 | 788.15 | 918.49 |
| Crystal system | Triclinic | Triclinic | Monoclinic |
| $a/\text{Å}$ | 7.143(1) | 14.376(4) | 8.539(4) |
| $b/\text{Å}$ | 7.846(2) | 15.510(5) | 14.605(7) |
| $c/\text{Å}$ | 25.714(5) | 15.595(5) | 32.070(16) |
| $\alpha/^\circ$ | 89.26(3) | 97.05(2) | 90 |
| $\beta/^\circ$ | 83.09(3) | 111.52(2) | 94.04(3) |
| $\gamma/^\circ$ | 66.50(3) | 97.34(1) | 90 |
| $U/\text{Å}^3$ | 1311.0 | 3153.7 | 3989.6 |
| $D_c/\text{g cm}^{-3}$ | 1.768 | 1.660 | 1.528 |
| $Z$ | 2 | 4 | 2 |
| Space group | $A\bar{1}$ [non-standard setting of $P\bar{1}$ (no. 2)] | $P\bar{1}$ (no. 2)] | $P2_1/c$ (no. 14) |
| Diffractometer | Siemens R3m/V | Stoë | Stoë |
| Colour | Red | Red | Red |
| Dimensions/mm | 0.1 × 0.4 × 0.6 | 0.22 × 0.28 × 0.34 | 0.15 × 0.15 × 0.61 |
| $F(000)$ | 684 | 1560 | 1848 |
| $\mu(\text{Mo-K}\alpha)/\text{cm}^{-1}$ | 25.42 | 21.23 | 17.16 |
| No. reflections used to determine cell | 25 | 50 | 50 |
| Data collection mode | $\omega$–2$\theta$ | $\omega$–$\theta$ | $\omega$–$\theta$ |
| Scan width/$^\circ$ | 1.20 + K$\alpha$ | 1.20 + K$\alpha$ | 0.90 + K$\alpha$ |
| Scan speed/$^\circ$ min$^{-1}$ | 3.00–19.53 | 0.90–3.60 | 0.60–2.40 |
| 2$\theta$ limits/$^\circ$ | 5–50 | 5–45 | 5–45 |
| Index limits | $+h, \pm k, \pm l$ | $\pm h, \pm k, -l$ | $+h, +k, \pm l$ |
| No. reflections measured | 4911 | 8620 | 2461 |
| Obs. reflections level $n[F > n\sigma(F)]$ | 4 | 4 | 5 |
| No. observed reflections | 1763 | 5547 | 1341 |
| Transmission factors min.–max. | 0.461–0.836 | 0.544–0.659 | 0.398–0.484 |
| $g$ in $w = 1/[\sigma^2(F_o) + gF_o^2]$ | 0.001 | 0.0028 | 0.0012 |
| $R$ | 0.046 | 0.056 | 0.056 |
| $R'$ | 0.048 | 0.057 | 0.059 |

**Table 7** Atomic coordinates ( × $10^4$) for complex **1**

| Atom | $x$ | $y$ | $z$ |
|---|---|---|---|
| Co(1) | 2760(1) | 3205(1) | 880(1) |
| Co(2) | 5583(1) | 1160(1) | 1354(1) |
| C(1) | 3353(11) | 691(9) | 1109(3) |
| C(2) | 2608(9) | 1860(8) | 1527(2) |
| C(3) | 1270(8) | 2204(7) | 2013(2) |
| C(4) | 689(10) | 804(8) | 2220(2) |
| C(5) | 561(10) | 3894(8) | 2298(3) |
| C(11) | 4323(13) | 2876(11) | 247(3) |
| O(11) | 5277(12) | 2688(10) | −145(2) |
| C(12) | 307(17) | 3727(15) | 678(4) |
| O(12) | −1232(13) | 4012(15) | 537(4) |
| C(13) | 2376(12) | 5481(10) | 1125(3) |
| O(13) | 2128(13) | 6890(8) | 1292(3) |
| C(21) | 7670(13) | 110(13) | 826(4) |
| O(21) | 8900(12) | −610(13) | 498(3) |
| C(22) | 5984(13) | 3025(13) | 1659(4) |
| O(22) | 6166(13) | 4246(12) | 1832(4) |
| C(23) | 6455(13) | −581(12) | 1840(4) |
| O(23) | 6927(12) | −1686(11) | 2135(3) |

undergoes oxidative addition of the Sn–C bond on reaction with $[Co_2(CO)_8]$. There is one report[14] which considers the preparation of a cobalt–diyne derivative involving a carbon–tin bond according to the reaction shown in equation (1).

$$2[Co_2(CO)_8] + Me_2Sn(C_2Ph)_2 \longrightarrow$$
$$[Me_2Sn\{Co_2(CO)_6C_2Ph\}_2] + 4CO \quad (1)$$
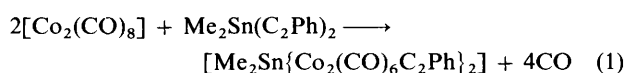
Unfortunately, no data supporting the characterisation of this tin complex were published since no crystalline product could be isolated. Therefore, the formation of $[\{Co_2(CO)_6\}_2(Me_3-SnC_2C_6H_4C_6H_4C_2SnMe_3)]$ appears to be the first preparation of a tin–alkyne cobalt carbonyl compound that can be characterised with only partial cleavage of the Sn–C bond.

## Experimental

Infrared spectra were recorded in NaCl cells (0.5 mm path length) on a Perkin Elmer PE983 or 1710FT spectrometer. Spectra of compounds in the solid state were recorded as pressed CsI discs (10 mm diameter). Electron impact (EI) mass spectra were recorded on either a Kratos MS902 or a AE1/Kratos MS12 spectrometer. Proton NMR spectra were recorded on a Bruker WH 250 (250 MHz) or on a WH 400 (400 MHz) Fourier transform spectrometer in the appropriate deuteriated solvent.

Dicobaltoctacarbonyl was obtained from Strem Chemicals and sublimed before use. The following diynes, $HC_2C_6H_4C_2H$, $HC_2C_6H_4C_6H_4C_2H$, $HC_2C_6H_4CH_2C_6H_4C_2H$, $Me_3SiC_2C_6-H_4C_6H_4C_2SiMe_3$ and $Me_3SiC_2C_6H_4CH_2C_6H_4C_2SiMe_3$ were prepared according to the method described by Hagihara and co-workers.[18] The diyne $Me_3SnC_2C_6H_4C_6H_4C_2SnMe_3$ was prepared in the manner described by Wright.[19] With the exception of the tin derivative **6**, which proved difficult to purify and always contained trace amounts of $HC_2C_6H_4C_6H_4C_2H$, there is close agreement between the published spectra and those recorded here.

*Preparations.*—$[\{Co_2(CO)_6\}_2(HC_2C_6H_4C_2H)]$ **1**. In a typical reaction, $[Co_2(CO)_8]$ (336 mg, 0.98 mmol) and $HC_2C_6-H_4C_2H$ (62 mg, 0.49 mmol) were dissolved in hexane (40 cm$^3$). The orange-brown solution was stirred at room temperature and the reaction monitored by IR spectroscopy. After 1 h the solution had changed in colour from orange to red and the infrared spectrum showed that the bridging carbonyls due to $[Co_2(CO)_8]$ had disappeared. The solution was filtered through a short column of Celite and the volume of the resulting solution was reduced to *ca.* 10 cm$^3$. Crystallisation at −25 °C yielded a reddish purple crystalline material (260 mg) which was separated by filtration at room temperature. Recrystallisation from hexane at 0 °C gave dark red crystals suitable for single-crystal X-ray analysis. IR (CsI): 2092m, 2060vs, 2033s, 2028w(sh), 2018w(sh) and 1987w cm$^{-1}$. Mass spectrum: $m/z$ 698

**Table 8** Atomic coordinates ( × $10^4$) for complex **3**

| Atom | $x$ | $y$ | $z$ | Atom | $x$ | $y$ | $z$ |
|---|---|---|---|---|---|---|---|
| Co(1) | 2 520(1) | 4 980(1) | 4 373(1) | Co(5) | 2 536(1) | 4 481(1) | 10 658(1) |
| Co(2) | 3 314(1) | 5 515(1) | 6 085(1) | Co(6) | 1 035(1) | 3 344(1) | 9 675(1) |
| C(101) | 3 345(9) | 4 204(8) | 4 303(8) | C(501) | 3 068(10) | 3 825(9) | 11 522(10) |
| O(101) | 3 894(8) | 3 738(6) | 4 303(7) | O(501) | 3 404(10) | 3 402(7) | 12 061(7) |
| C(102) | 2 971(8) | 5 909(8) | 3 926(8) | C(502) | 3 680(12) | 5 106(10) | 10 729(10) |
| O(102) | 3 233(8) | 6 471(5) | 3 623(7) | O(502) | 4 418(9) | 5 462(8) | 10 688(11) |
| C(103) | 1 396(11) | 4 476(9) | 3 381(10) | C(503) | 2 025(10) | 5 300(9) | 11 211(10) |
| O(103) | 644(9) | 4 207(9) | 2 761(7) | O(503) | 1 657(10) | 5 806(8) | 11 512(7) |
| C(201) | 4 313(8) | 4 872(7) | 6 406(7) | C(601) | 70(9) | 2 898(8) | 8 559(9) |
| O(201) | 4 942(6) | 4 479(5) | 6 620(7) | O(601) | −560(6) | 2 636(7) | 7 822(6) |
| C(202) | 3 998(8) | 6 605(7) | 6 114(7) | C(602) | 1 424(8) | 2 343(8) | 10 045(8) |
| O(202) | 4 404(6) | 7 280(5) | 6 126(6) | O(602) | 1 698(7) | 1 708(6) | 10 252(7) |
| C(203) | 3 126(8) | 5 691(7) | 7 147(8) | C(603) | 195(9) | 3 364(7) | 10 243(8) |
| O(203) | 2 943(8) | 5 796(5) | 7 798(6) | O(603) | −292(7) | 3 880(7) | 10 630(7) |
| C(1) | −207(6) | 1 565(5) | 5 896(6) | C(18) | 4 703(7) | 2 366(6) | 7 595(6) |
| C(2) | 388(6) | 2 392(5) | 5 763(5) | C(19) | 4 024(6) | 2 724(6) | 8 050(6) |
| C(3) | 1 142(6) | 2 322(5) | 5 420(6) | C(20) | 3 336(6) | 3 244(6) | 7 636(6) |
| C(4) | 1 660(6) | 3 068(5) | 5 260(6) | C(21) | 2 752(6) | 3 583(5) | 8 067(6) |
| C(5) | 1 455(5) | 3 901(5) | 5 472(5) | C(22) | 2 847(6) | 3 428(5) | 8 947(6) |
| C(6) | 714(6) | 3 960(5) | 5 832(6) | C(23) | 3 522(6) | 2 890(5) | 9 365(6) |
| C(7) | 194(6) | 3 222(5) | 5 972(6) | C(24) | 4 097(6) | 2 555(6) | 8 920(6) |
| C(8) | 2 014(6) | 4 686(5) | 5 325(5) | C(25) | 2 227(6) | 3 794(5) | 9 397(6) |
| C(9) | 1 940(6) | 5 514(6) | 5 212(6) | C(26) | 1 622(7) | 4 401(6) | 9 351(6) |
| C(10) | 428(6) | 986(5) | 6 494(6) | C(27) | 4 145(6) | 1 869(6) | 6 603(6) |
| C(11) | 190(6) | 66(5) | 6 206(6) | C(28) | 4 402(7) | 2 111(6) | 5 875(7) |
| C(12) | 738(6) | −471(5) | 6 753(6) | C(29) | 3 945(7) | 1 644(6) | 4 981(6) |
| C(13) | 1 529(6) | −136(5) | 7 604(6) | C(30) | 3 163(6) | 917(5) | 4 742(6) |
| C(14) | 1 751(6) | 791(6) | 7 910(6) | C(31) | 2 866(6) | 689(5) | 5 463(6) |
| C(15) | 1 200(6) | 1 328(5) | 7 348(6) | C(32) | 3 342(6) | 1 156(6) | 6 359(7) |
| C(16) | 2 140(6) | −698(5) | 8 175(6) | C(33) | 2 684(6) | 390(5) | 3 802(6) |
| C(17) | 2 788(7) | −735(6) | 9 046(6) | C(34) | 1 892(6) | −212(6) | 3 232(6) |
| Co(3) | 1 928(1) | −1 881(1) | 8 463(1) | Co(7) | 3 114(1) | −562(1) | 3 154(1) |
| Co(4) | 3 347(1) | −1 158(1) | 8 121(1) | Co(8) | 2 231(1) | 617(1) | 2 517(1) |
| C(301) | 887(8) | −1 786(7) | 8 797(7) | C(701) | 4 430(8) | −40(7) | 3 478(7) |
| O(301) | 222(6) | −1 701(6) | 9 032(6) | O(701) | 5 235(6) | 333(6) | 3 691(7) |
| C(302) | 2 563(8) | −2 578(7) | 9 288(8) | C(702) | 2 702(9) | −1 352(8) | 2 056(9) |
| O(302) | 2 977(7) | −2 965(6) | 9 823(6) | O(702) | 2 422(9) | −1 804(7) | 1 355(6) |
| C(303) | 1 290(8) | −2 625(7) | 7 337(8) | C(703) | 3 243(8) | −1 312(7) | 3 960(8) |
| O(303) | 921(7) | −3 084(5) | 6 631(6) | O(703) | 3 274(9) | −1 757(6) | 4 476(7) |
| C(401) | 4 170(8) | −1 933(7) | 8 538(7) | C(801) | 1 231(11) | 31(9) | 1 429(11) |
| O(401) | 4 677(6) | −2 432(5) | 8 769(6) | O(801) | 590(11) | −364(8) | 789(8) |
| C(402) | 4 307(9) | −221(8) | 8 402(8) | C(802) | 3 231(10) | 1 089(8) | 2 209(9) |
| O(402) | 4 931(7) | 394(6) | 8 637(7) | O(802) | 3 878(8) | 1 375(7) | 1 995(8) |
| C(403) | 2 864(8) | −1 423(7) | 6 849(8) | C(803) | 1 774(9) | 1 601(8) | 2 779(8) |
| O(403) | 2 520(6) | −1 590(6) | 6 068(5) | O(803) | 1 505(8) | 2 212(6) | 3 000(7) |

(Found: C, 37.9; H, 0.85. Calc. for $C_{22}H_6Co_4O_{12}$: C, 37.7; H, 0.90%).

[{$Co_2(CO)_6$}$_2$($HC_2C_6H_4C_6H_4C_2H$)] **2**. Octacarbonyldicobalt(0) (200 mg, 0.58 mmol) and $HC_2C_6H_4C_6H_4CC_2H$ (60 mg, 0.29 mmol) were dissolved in hexane (40 cm$^3$). The solution was heated at 40 °C for 20 min. The solution was separated on a silica gel (mesh 70–230 mm) column using hexane–$CH_2Cl_2$ (75:25) as eluent. Only one red band was collected. Crystallisation at −25 °C yielded a reddish purple crystalline material (180 mg). IR (CsI): 2094m, 2058vs, 2032s, 2028w(sh), 2018w(sh) and 1987w cm$^{-1}$ (Found: C, 43.4; H, 1.30. Calc. for $C_{28}H_{10}Co_4O_{12}$: C, 43.7; H, 1.40%).

[{$Co_2(CO)_6$}$_2$($HC_2C_6H_4CH_2C_6H_4C_2H$)] **3**. Compound **3** was prepared on a 0.15 mmol scale by the same method described for **2**. The solution was filtered through a short column of Celite and reduced in volume to ca. 10 cm$^3$. The first red band was collected and crystallisation at −25 °C yielded a reddish purple crystalline material (70 mg). Recrystallisation from hexane at −25 °C gave large hexagonal crystals which on cutting were suitable for single-crystal X-ray diffraction analysis. IR (CsI): 2094m, 2057vs, 2031vs, 2027s(sh), 2016m and 1986w cm$^{-1}$. Mass spectrum: $m/z$ 788 (Found: C, 44.2; H, 1.55. Calc. for $C_{29}H_{12}Co_4O_{12}$: C, 44.3; H, 1.55%).

[{$Co_2(CO)_6$}$_2$($Me_3SiC_2C_6H_4C_6H_4C_2SiMe_3$)] **4**. Compound **4** was prepared on a 0.30 mmol scale by the same method described for **2**. The solution was filtered through a Celite column and reduced in volume to ca. 10 cm$^3$. Crystallisation at −25 °C yielded a dark purple crystalline material (115 mg). Recrystallisation by slow layer diffusion of hexane into a hexane–$CH_2Cl_2$ mixture at 0 °C gave hexagonal purple crystals of **4** suitable for single crystal X-ray diffraction analysis. IR (CsI): 2087m, 2053vs, 2026s, 2022s(sh), 2010w and 1977w cm$^{-1}$ (Found: C, 44.5; H, 2.85. Calc. for $C_{34}H_{26}Co_4O_{12}Si_2$: C, 44.3; H, 2.75%).

[{$Co_2(CO)_6$}$_2$($Me_3SiC_2C_6H_4CH_2C_6H_4C_2SiMe_3$)] **5**. Complex **5** was prepared on a 0.30 mmol scale by the same method described for **2**. The solution was filtered through a Celite column and reduced in volume to ca. 10 cm$^3$. Crystallisation at −25 °C yielded a dark purple crystalline material (115 mg). IR (CsI): 2088m, 2052vs, 2026vs, 2021vs(sh), 2009w and 1976w(sh) cm$^{-1}$. Mass spectrum: $m/z$ 876 (Found: C, 45.1; H, 3.0. Calc. for $C_{23}H_{28}Co_4O_{12}Si_2$: C, 45.1; H, 3.15%).

[{$Co_2(CO)_6$}$_2$($Me_3SnC_2C_6H_4C_6H_4C_2SnMe_3$)] **6**. Complex **6** was prepared on a 0.30 mmol scale by the method described for **1**. The solution was filtered through a column of Celite and reduced in volume to ca. 10 cm$^3$. Crystallisation at −25 °C

**Table 9** Atomic coordinates ( × $10^4$) for complex **4**

| Atom | x | y | z |
|---|---|---|---|
| Co(1) | −586(2) | 691(1) | 920(1) |
| Co(2) | 1 193(2) | 1 417(1) | 1 467(1) |
| C(1) | −530(12) | 1 997(5) | 1 101(2) |
| C(2) | −1 109(10) | 1 474(5) | 1 395(3) |
| Si(1) | −668(4) | 3 077(2) | 800(1) |
| C(3) | −2 710(20) | 3 143(8) | 539(4) |
| C(4) | 807(16) | 3 084(7) | 403(3) |
| C(5) | −386(20) | 4 062(7) | 1 168(4) |
| C(6) | −2 295(12) | 1 448(5) | 1 700(2) |
| C(7) | −3 016(12) | 2 246(6) | 1 814(3) |
| C(8) | −4 111(13) | 2 238(6) | 2 121(3) |
| C(9) | −4 446(11) | 1 457(5) | 2 328(3) |
| C(10) | −3 687(13) | 634(6) | 2 211(3) |
| C(11) | −2 691(12) | 629(6) | 1 905(3) |
| C(12) | −2 409(15) | 672(6) | 618(3) |
| C(13) | −620(12) | −462(6) | 1 132(3) |
| C(14) | 753(14) | 655(6) | 502(3) |
| C(15) | 1 511(16) | 2 324(9) | 1 841(3) |
| C(16) | 1 505(17) | 418(9) | 1 786(4) |
| C(17) | 2 958(15) | 1 554(7) | 1 179(4) |
| O(1) | −3 615(10) | 657(6) | 423(3) |
| O(2) | −681(14) | −1 174(5) | 1 265(3) |
| O(3) | 1 571(12) | 634(5) | 241(3) |
| O(4) | 1 629(18) | 2 897(8) | 2 080(3) |
| O(5) | 1 642(19) | −223(7) | 1 989(3) |
| O(6) | 4 068(12) | 1 648(6) | 1 011(3) |

yielded a dark reddish brown crystalline material (138 mg) identified by spectroscopic methods as the diyne complex **6**. IR (CsI): 2094m, 2058s, 2032m(sh), 2018s(sh) and 1987w(sh) cm$^{-1}$ (Found: C, 37.1; H, 2.40. Calc. for $C_{22}H_{26}Co_4O_{12}Sn_2$: C, 38.4; H, 2.45%).

*Crystal Structure Determination and Refinements.*—Suitable crystals of the compounds were mounted on glass fibres with epoxy resin. Details of crystal data, data collection and refinement parameters are given in Table 6.

The cobalt atoms in each of the three structures were located by centrosymmetric direct methods, and the remaining non-hydrogen atoms from subsequent Fourier difference syntheses. The hydrogen atoms were placed in idealised positions (C–H 0.96 Å) and allowed to ride on the relevant carbon atoms; for structures **1** and **3** the hydrogen atom displacement parameter was fixed at 0.08 Å$^2$, while for structure **4** the methyl and phenyl hydrogen displacement parameters refined to 0.14(2) and 0.07(1) Å$^2$, respectively. The structures were refined to convergence by full-matrix least squares with all non-hydrogen atoms assigned anisotropic displacement parameters for **1** and **4**, and with all but the carbonyl carbons anisotropic for **3**. Weighting schemes were applied, and analyses of the variations of the sum of $w\Delta^2$ ($\Delta = F_o - |F_c|$) according to $|F_o|$ and sin θ indicated that the schemes were appropriate. The final residuals were calculated on the basis $R = [\Sigma|F_o - |F_c||/\Sigma F_o]$, $R' = [\Sigma w^{\frac{1}{2}}|F_o - |F_c||/\Sigma w^{\frac{1}{2}}F_o]$, and $w = 1/[\sigma^2(F_o) + gF_o^2]$ where $\sigma(F_o)$ is calculated from counting statistics. Final electron density difference maps showed no regions of significant electron density. The final positional coordinates for all the non-hydrogen atoms in **1**, **3** and **4** are listed in Tables 7–9, respectively. All atoms were assigned neutral-atom scattering factors which were taken from ref. 20. Calculations were performed on the University of Cambridge IBM 3084Q mainframe computer using SHELX 76,[21] for **4**, and on a MicroVax II computer using the SHELXTL PLUS package,[22] for **1** and **3**.

Additional material available from the Cambridge Crystal-lographic Data Centre comprises H-atom coordinates, thermal parameters, and remaining bond lengths and angles.

*Molecular Orbital Calculations.*—Fenske-Hall[23] calculations used the crystallographically determined coordinates for **1**. Single-ζ Slater functions were employed for the 1s and 2s functions of C and O. The exponents were obtained by curve fitting the double-ζ functions of Clementi[24] while maintaining orthogonal functions. The double-ζ functions were used directly for the 2p orbitals. An exponent of 1.16 was used for hydrogen. The basis functions for cobalt were chosen for the (+1) oxidation state and were taken from results of Richardson *et al.*[25] and augmented by 4s and 4p functions with exponents of 2.0. For the calculations, a model cluster $[Co_2(CO)_6(HCCPh)]$ was used with structural parameters taken not from the compounds reported here but adapted from the symmetrically substituted cluster $[Co_2(CO)_6(PhCCPh)]$.[1] The model cluster was given Co–C bond lengths of 1.95 Å. The coordinates of the phenyl substituent in the model were taken directly from those of one substituent in $[Co_2(CO)_6(PhCCPh)]$ while the C–H group was located with the C–H vector coincident with the second C–$C_{ipso}$ vector of $[Co_2(CO)_6(PhCCPh)]$ and $d_{C-H} = 1.02$ Å. A value of $d_{CC} = 1.36$ Å was used.

## References
1 B. F. G. Johnson, J. Lewis, P. R. Raithby and D. A. Wilkinson, *J. Organomet. Chem.*, 1991, **408**, C9.
2 D. Seyferth and H. P. Withers, *Inorg. Chem.*, 1983, **22**, 2931.
3 P. Magnus and D. P. Becker, *J. Chem. Soc., Chem. Commun.*, 1985, 640.
4 Y. Rubin, C. B. Knobler and F. Diederich, *J. Am. Chem. Soc.*, 1990, **112**, 4966.
5 G. Cetini, O. Gambino, R. Rosetti and E. Sappa, *J. Organomet. Chem.*, 1967, **8**, 149.
6 W. Sly, *J. Am. Chem. Soc.*, 1959, **81**, 18; D. A. Brown, *J. Chem. Phys.*, 1960, **33**, 1037.
7 D. Gregson and J. A. K. Howard, *Acta Crystallogr., Sect. C*, 1983, **39**, 1024.
8 F. A. Cotton, J. D. Jamerson and B. J. Stults, *J. Am. Chem. Soc.*, 1976, **98**, 1774.
9 G. G. Summer, H. P. Klug and L. E. Alexander, *Acta Crystallogr.*, 1964, **17**, 732.
10 S. Aime, L. Milone, R. Rossetti and P. L. Stanghellini, *Inorg. Chim. Acta*, 1977, **22**, 135.
11 R. K. Harris, *Nuclear Magnetic Resonance Spectroscopy: A Physiochemical View*, Pitman, London, 1983.
12 D. H. Williams and I. Fleming, *Spectroscopic Methods in Organic Chemistry*, McGraw-Hill, London, 1980.
13 K. H. Pannell and G. M. Crawford, *J. Coord. Chem.*, 1973, **2**, 251.
14 S. D. Ibekwe and M. J. Newlands, *J. Chem. Soc., Sect. A*, 1967, 1783.
15 R. L. DeKock, P. Deshmukh, T. K. Dutta, T. P. Fehlner, C. E. Housecroft and J. L.-S. Hwang, *Organometallics*, 1983, **2**, 1108.
16 D. L. Thorn and R. Hoffmann, *Inorg. Chem.*, 1978, **7**, 126.
17 M. F. Lappert, B. Cetinkaya, J. McMeeking and D. E. Palmer, *J. Chem. Soc., Dalton Trans.*, 1973, 1202.
18 S. Takahashi, Y. Yuroyama, K. Sonogashira and N. Hagihara, *Synthesis*, 1980, 627.
19 M. E. Wright, *Macromolecules*, 1989, **22**, 3256.
20 *International Tables for X-Ray Crystallography*, Kynoch Press, Birmingham, 1974, vol. 4.
21 G. M. Sheldrick, SHELX 76, Crystal Structure Determination Package, University of Cambridge, 1976.
22 Release 4.0 of SHELXTL PLUS, Siemens Part No. 269-004200, Siemens Analytical X-Ray Instruments, Madison, 1990.
23 M. B. Hall and R. F. Fenske, *Inorg. Chem.*, 1972, **11**, 768.
24 E. Clementi, *J. Chem. Phys.*, 1964, **40**, 1944.
25 J. W. Richardson, W. C. Nieuport, R. R. Powell and W. F. Edgell, *J. Chem. Phys.*, 1962, **36**, 1057.